Step-Scan FT-IR Monitoring of Transient HCO Radicals in a Room Temperature Zeolite

Y. H. Yeom and H. Frei*

Physical Biosciences Division, Mailstop Calvin Laboratory, Lawrence Berkeley National Laboratory, University of California, Berkeley, California 94720

Received: November 8, 2002; In Final Form: April 18, 2003

Formyl radical has been detected in zeolite NaY at room temperature by step-scan FT-infrared spectroscopy upon photodissociation of glycolaldehyde or acetaldehyde precursor. Identification was made by the C═O stretch absorption at 1847 cm^{-1} and a ^{13}C isotope shift of 40 cm^{-1}. The decay shows biphasic kinetics independent of the precursor used. In the case of glycolaldehyde, the final products recorded by static FT-IR spectroscopy can be explained by the exclusive reaction of HCO and CH_2OH radicals. This allowed us to assign the initial decay with a lifetime of 24 ± 3 μs to geminate reactive encounters of HCO and CH_2OH radicals. The subsequent long tail extending to 500 μs is well described by a second-order rate law consistent with nongeminate reaction of the radicals. This is the first direct kinetic observation of geminate and nongeminate radical reactions in a zeolite.

Introduction

Detection of small transient radicals in microporous solids is the key to a mechanistic understanding of chemical reactions in these important catalytic materials. In a recent study of pinacolone and 1-naphthyl acetate photodissociation in solvent-free NaY at room temperature by step-scan FT-IR spectroscopy, we have been able to detect the first small transient radical in a zeolite.[1−3] In parallel work on photoactivation of CO in another microporous solid (Ti silicalite) using methanol as a donor, results point to formyl radical as reaction intermediate.[4] In light of these results, and the proposed mechanistic role of formyl radicals in important catalytic processes on solid supports,[5] including zeolites, we have attempted to generate and detect HCO radicals in a zeolite by photodissociation of a stable precursor with the goal of learning about the behavior of such a small radical in an ambient microporous environment. In addition to developing a capability of detecting HCO radical intermediate under reaction conditions, it is very interesting to know whether in a given zeolite environment the fate of HCO differs from that of the previously studied CH_3CO radical. For example, is the unexpected long lifetime of acetyl radical of tens of microseconds (naphthyl acetate precursor) to hundreds of microseconds (pinacolone precursor) in NaY a special case that applies only to these systems?[1−3] There is even the question of whether the lifetime of a triatomic radical like HCO is sufficiently long to allow detection by time-resolved FT-IR spectroscopy. Furthermore, does the formyl radical exhibit a similar fate in a zeolite as the acetyl radical, which is characterized by separation of the radical pair from the cage in which precursor photolysis took place, followed by random walk and chemical reaction upon encounter with a geminate partner?[2,3] The latter behavior was manifested by single-exponential decay kinetics of the acetyl radical.

To address these questions, we have searched for HCO radicals by step-scan FT-IR spectroscopy of the photodissociation of two alternate HCO precursors in zeolite NaY at room temperature, namely glycolaldehyde and acetaldehyde. Complete final product assignment based on static FT-IR results could be made in the case of glycolaldehyde dissociation, but not for acetaldehyde photolysis. Therefore, the main emphasis of the discussion is on the results obtained using glycolaldehyde as a precursor.

Experimental Section

Time-resolved and static FT-IR spectra were recorded on a step-scan spectrometer Bruker model IFS88 described previously.[1,2,6] The instrument was equipped with an HgCdTe PV detector Kolmar Technologies model KMPV8−1-J2 (fwhm = 37 ns, RC decay of AC preamplifier = 1.4 ms). For step-scan runs on the nanosecond time scale with sampling intervals of 25 ns, AC and DC-coupled interferometric signals were simultaneously acquired by a 40 MHz 12 bit digitizer (model PAD 1232). Prior to digitization, the AC-coupled signal was amplified by a factor of 100 (CAL-AV Laboratories model 7930 500 MHz amplifier), while the DC-coupled signal was amplified by a factor of 2 or 5 after adjusting the offset to ground (LeCroy model 6103 programmable amplifier). The amplification assured use of the full dynamic range (±1V) of the digitizer. For step-scan measurements on the μs time scale with 5 μs intervals, a 200 kHz 16-bit digitizer was employed. Prior to recording the AC-coupled interferogram, a DC-coupled step-scan run was conducted (without sample excitation) to obtain a phase spectrum. The latter was stored for subsequent use in the Fourier transformation of the AC-coupled interferograms. Transient absorbance difference spectra were computed as

$$\Delta A = -\log\frac{(S + \Delta S)}{S}$$

(S, static single beam spectrum = FT of DC-coupled interferogram; ΔS, laser-induced spectrum = FT of AC-coupled interferogram).

Glycolaldehyde samples were photolyzed with 266 nm pulses (5 ns fwhm) of an Nd:YAG laser model Quanta Ray DCR-2A (with GRC-3 upgrade). For photodissociation of acetaldehyde, the second harmonic output of the PDL-1 dye laser was used

* To whom correspondence should be addressed. E-mail: hmfrei@lbl.gov.

10.1021/jp022394h CCC: $25.00
Published on Web 06/07/2003

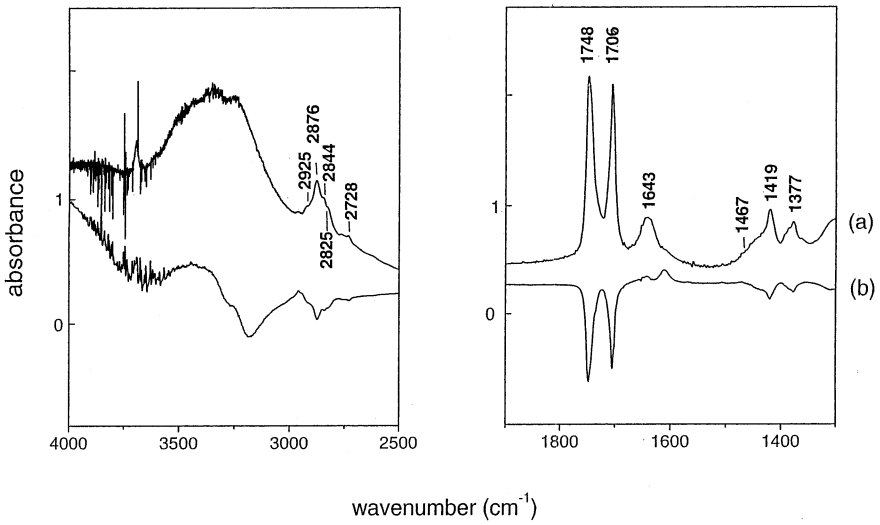

Figure 1. (a) FT-IR spectrum of glycolaldehyde adsorbed onto dehydrated NaY. (b) Difference spectrum upon 15 min irradiation at 266 nm at 4.2 mJ cm^{-2} $pulse^{-1}$ (10 Hz).

(290 nm). The dye laser was pumped by the 532 nm emission of the Nd:YAG laser. The laser emission consisted of 5 mJ cm^{-2} pulses at 10 Hz repetition rate. The photolysis beam was aligned collinearly with the FT-IR probe beam by a small (1 cm edge-to-edge) UV grade fused silica prism. To prevent scattered photolysis light from reaching interferometer and detector optics, AR-coated Ge plates (International Scientific, 96% transmittance) were placed in the openings of the interferometer and detector compartments. Data acquisition was triggered by a small fraction of the photolysis laser pulse detected by an EG&G Si photodiode, model SGD-444.

Folding limits for step-scan measurements were 2430 and 1823 cm^{-1} or 2060−1718 cm $^{-1}$, depending on whether the infrared filter W04684−4 or W05342−8 (Optical Coating Laboratory) was used. Filters were installed in front of the infrared detector. Spectral resolution was 4 cm^{-1}, resulting in step-scan runs of 307 mirror positions (2430−1823 cm^{-1}) or 173 mirror positions (2060−1718 cm^{-1}), respectively. At each mirror position, 15 laser-induced decays (2430−1823 cm^{-1}) or 25 laser-induced decays (2060−1718 cm $^{-1}$) were recorded and averaged. All experiments were conducted at room temperature.

UV−Vis diffuse reflectance spectra of pressed NaY pellets were measured with a Shimadzu model UV-2100 spectrometer equipped with an integrating sphere model ISR-260.

Self-supporting wafers of 7−10 mg zeolite NaY crystallites (Aldrich, LZ-Y52, Lot. No. 12929CN) were prepared in a KBr press and placed inside a miniature infrared vacuum cell. The evacuated cell (Varian turbomolecular pump Model V-70) was heated in a Glas-Col heating mantle to 473 K, and the zeolite pellet was dehydrated for 12 h.

Two different procedures were employed for the loading of glycolaldehyde. The first method consisted of stirring 0.7 g of dehydrated NaY powder in a solution of 40 mg glycolaldehyde (Fluka, 98%) in 25 mL of THF (Aldrich, 99.9%) for 3 h at 22 °C inside a drybox. The supernatant solution was decanted, the zeolite was washed with fresh THF, and the wet NaY powder was pressed into a pellet. Evacuation of the wafer at 70 °C inside the infrared cell for 1 h completely removed the solvent. The second method did not employ any solvent. It consisted of dehydration of a pressed NaY pellet in the IR cell at 200 °C for 10 h. After cooling to RT, approximately 1 mg glycolaldehyde was placed into the infrared cell in a drybox, and the cell was evacuated and heated for 1 h at 70 °C. Infrared spectra indicated that this method resulted in high loading of the pellet by monomeric glycolaldehyde. Authentic samples of reaction products methanol (99.8%, EM Science), carbon monoxide (99.99%, Matheson), methane (99.97%, Matheson), and methyl formate (99%, Aldrich) were used as received. A sample of partially labeled $HOCH_2CH{=}^{18}O$ was prepared by exchange of the parent glycolaldehyde in $H_2{}^{18}O$ for 24 h at room temperature. $^{12}C_2$ -acetaldehyde (Aldrich, 99%) or $^{13}C_2$ -acetaldehyde (Cambridge Isotope Laboratories, 99% ^{13}C) was loaded into the dehydrated zeolite pellet from the gas phase. The pressure was 1.5 Torr, resulting in a loading level of 4 to 5 molecules per supercage.

Results

Photodissociation of Glycolaldehyde. The FT-IR spectrum of monomeric glycolaldehyde adsorbed onto dehydrated NaY sieve shows absorptions at 1377, 1419, 1467(sh), 1705, 1748, 2728, 2825(sh), 2844(sh), 2876, 2925(sh), and 3350 cm^{-1} (very broad) (Figure 1a), which is in good agreement with gas phase and matrix isolation infrared spectra reported in the literature.[7−9] Interestingly, there are two strong bands observed for glycoaldehyde in NaY in the 1700−1750 cm^{-1} region, shown on an expanded scale in Figure 2a. Spectra of a partially labeled $HO{-}CH_2{-}CH{=}^{18}O$ sample in NaY revealed new peaks at 1725 and 1680 cm^{-1} (Figure 2b). Since both new bands exhibit the same characteristic red shift of a C═O group upon ^{18}O substitution of the carbonyl oxygen, they are assigned to two different sites of $HO{-}CH_2{-}CH{=}O$ in a NaY sieve. The isotope shift rules out alternative assignment of the 1705 cm^{-1} feature to the C═C stretching mode of the $HO{-}CH{=}CH{-}OH$ tautomer, which would absorb at the same frequency.[10] Aside from a small amount of coadsorbed H_2O signaled by the bending absorption at 1643 cm^{-1}, no impurity was detected. Photolysis at 266 nm resulted in efficient depletion of the aldehyde under concurrent growth at 1435, 1455, 1471, 1505, 1605, 2850, 2958, and 3400 cm^{-1} (broad). Static FT-IR difference spectra following 15 min irradiation (4.2 mJ cm^{-2} $pulse^{-1}$, 10 Hz) are shown in trace b of Figure 1, and on an expanded scale, in Figure 3. Assignments are readily made based on comparison with spectra of authentic samples, namely, CH_3OH (1353, 1455, 1471, 2850, 2958, 3400 cm^{-1}), CO (gas-phase spectrum in the 2000−2200 cm^{-1} region), $CH_2{=}O$ (1505 cm^{-1}), HCO_2CH_3 (1435, 1455 cm^{-1}), and HCO_2^-(1605 cm^{-1}). These photolysis products are consistent with the UV photodissociation products of glycolaldehyde in

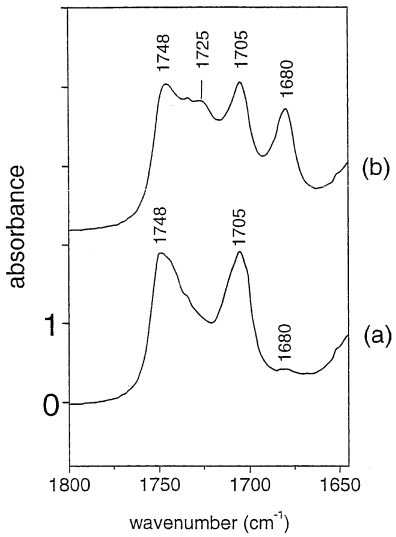

Figure 2. C═O stretching region of glycolaldehyde in NaY. (a) HO−CH_2−CH═O; (b) partially HO−CH_2−CH═^{18}O labeled glycolaldehyde sample.

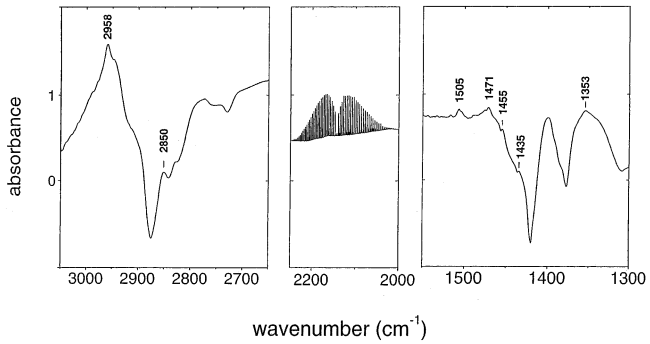

Figure 3. FT-IR difference spectrum before and after 15 min irradiation at 266 nm at 4.2 mJ cm^{-2} $pulse^{-1}$ (10 Hz) recorded at 0.25 cm^{-1} resolution.

gas phase and solution, namely, methanol, CO, and formaldehyde.[8,11,12] Additional products HCO_2CH_3 and HCO_2^- observed here are expected from secondary thermal reactions of CH_2═O as both Tishchenko dimerization and Cannizzaro reaction with residual H_2O have been observed previously in other microporous solids.[13,14] The UV diffuse reflectance spectrum of glycoaldehyde-loaded NaY with its nπ^* absorption at 280 nm, shown in Figure 4, agrees well with gas-phase spectra reported in the literature.[11,12]

Step-scan spectra of 266 nm photodissociation of $HOCH_2$-CH═O revealed a transient absorption at 1847 cm^{-1}, shown in Figure 5a. The signal represents the average of the 5 μs spectra of 24 step-scan runs. The 250 μs trace constitutes a time average from 200 to 300 μs after the photolysis pulse (coaddition of 20 5 μs time slices). The infrared frequency of the transient is very close to the C═O stretch of gas phase formyl radical at 1868 cm^{-1} [15] (1860 cm^{-1} in a cryogenic CO matrix).[16,17] The decay at 295 K, shown in Figure 5b, exhibits biphasic behavior. The initial decay (0−30 μs) is well described by a single-exponential law

$$A_t = A_0 e^{-k_1 t}$$

with $k_1 = (4.2 \pm 0.5)\ 10^4$ sec^{-1}. For reasons presented in the Discussion Section, data for 30 $\mu s < t < 500$ μs were fitted to

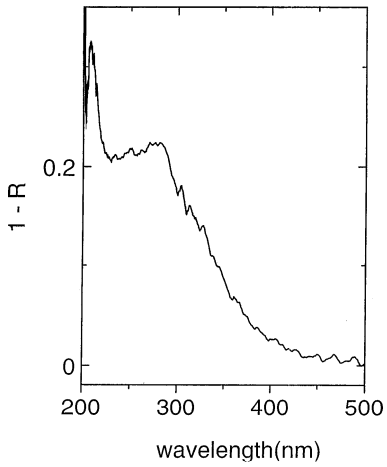

Figure 4. UV diffuse reflectance spectrum of glycolaldehyde loaded in NaY.

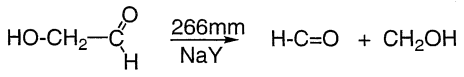

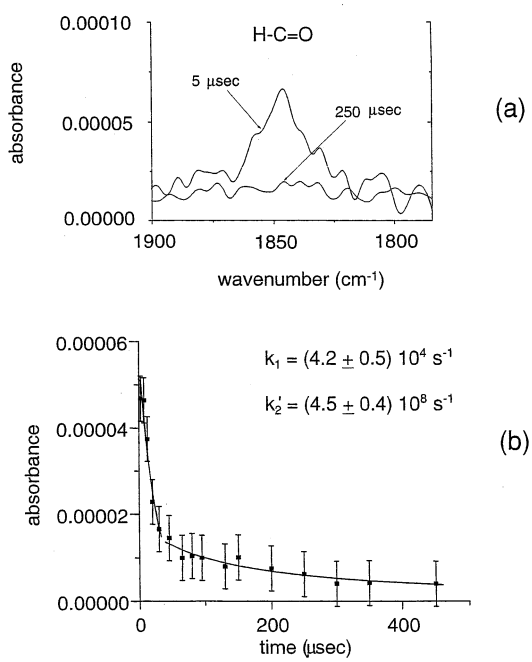

Figure 5. (a) Step-scan FT-IR spectra of glycolaldehyde photodissociation initiated by 266 nm laser pulses of 8 ns duration at room temperature. The 5 μs time slice represents the average of the corresponding time slice of 24 step-scan runs. The 250 μs trace represents the coaddition of twenty 5 μs time slices in the 200−300 μs interval. (b) Decay of the 1847 cm^{-1} transient.

a second-order rate law with reactants of equal concentration[18]

$$\frac{1}{A_t} = k_2' t + \frac{1}{A_0}$$

A least-squares fit gave $k_2' = (4.5 \pm 0.4)\ 10^8$ sec^{-1}. Experiments are limited to very small transient signals (4×10^{-5} absorbance units) due to the maximum affordable laser excitation pulse energy being 5 mJ; higher pulse energies with pressed zeolite wafers lead to large noise amplitudes, which currently prevents a laser intensity study of the decay kinetics.

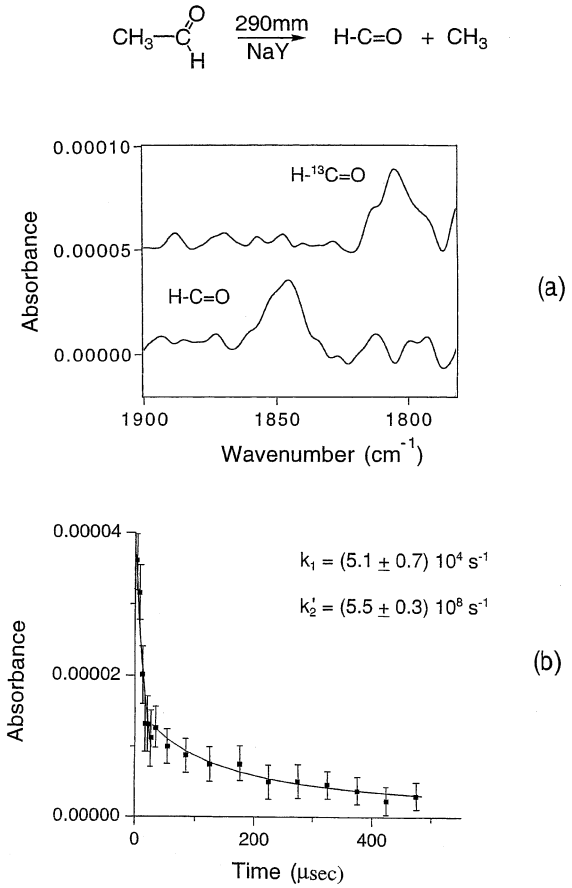

Figure 6. (a) Step-scan FT-IR spectra of acetaldehyde and $^{13}CH_3{}^{13}CH{=}O$ photodissociation by 290 nm laser pulses of 8 ns duration at room temperature. The spectra were recorded at 25 ns resolution and represent the coaddition of 200 time slices over the first 5 μs after the photolysis pulse. Details of the measurements are described in the text. (b) Decay of the 1845 cm^{-1} transient.

Photodissociation of Acetaldehyde. The identification of the transient as HCO was confirmed by generating the radical in zeolite NaY from an alternative precursor, acetaldehyde. Figure 6a shows a transient absorption with a peak at 1845 cm^{-1} upon 290 nm photolysis of $CH_3CH{=}O$, at 1805 cm^{-1}, when using $^{13}CH_3{}^{13}CH{=}O$ as a precursor. The spectra were recorded with the 40-MHz digitizer and represent the coaddition of 200 time slices over the first 5 μs after the photolysis pulse. Data of 120 step-scan runs were averaged in the case of the parent isotope, while 80 runs were used for the $^{13}CH_3{}^{13}CH{=}O$ sample. The observed ^{13}C isotope shift agrees well with the known shift of gas-phase $H^{13}CO$ radical.[15] On the basis of the agreement of the transient infrared band detected upon photolysis of glycolaldehyde and acetaldehyde, we conclude that the 1847 cm^{-1} species is the HCO radical. As in the case of $HOCH_2CH{=}O$, the formyl radical generated by photolysis of $CH_3CH{=}O$ exhibits a fast and slow decay with similar amplitudes and decay constants, as shown in Figure 6b ($k_1 = (5.1 \pm 0.7)\ 10^4\ sec^{-1}$, $k_2' = (5.5 \pm 0.3)\ 10^8\ sec^{-1}$). However, unlike the case of glycolaldehyde precursor, we were unable to unambiguously identify the stable products of acetaldehyde photolysis in NaY.

Discussion

The behavior of HCO radicals in zeolite NaY at room temperature revealed by the time-resolved measurements has two remarkable aspects. One is the unexpected long lifetime of these small radicals, the other, the biphasic nature of the decay. These features will be discussed in turn.

The nascent HCO + CH_2OH radical pair produced by photolysis of glycolaldehyde is most probably a spin triplet, because the precursor is known to dissociate from the T_1 state in aqueous solution.[19] Similarly, HCO and CH_3, the main fragmentation products of acetaldehyde photolysis at 290 nm,[20−24] are expected to emerge as a triplet pair.[25] The spin flip required for geminate radical reaction is known to proceed in a zeolite cage within nanoseconds.[26] Nevertheless, instant cage recombination does not occur for the majority of the pairs; because the residence time of an HCO radical is estimated to be about one ns (see below), the tens to hundreds of microsecond lifetime of HCO implies that the geminate HCO and CH_2OH (or CH_3) radicals separate from the supercage in which the precursor was photolyzed and undertake random walks until a reactive encounter occurs. Factors that favor separation of the radicals over instantaneous reaction in the cage include the availability of four large window openings of the supercage for escape and electrostatic or H-bonding interactions of the radicals with extraframework Na ions or the negatively charged cage walls.

Observation of CO, CH_3OH, $CH_2{=}O$, and HCO_2CH_3 and HCO_2^- (the latter two products resulting from subsequent thermal reaction of formaldehyde) as the exclusive final photolysis products of glycolaldehyde allows us to explain the biphasic behavior of the HCO decay kinetics. As shown in Scheme 1, CO and CH_3OH could be formed by H transfer from HCO to CH_2OH, while $CH_2{=}O$ may emerge from H transfer from CH_2OH to HCO. With the total rate of radical decay equal to the sum of the rates of the two competing HCO + CH_2OH reaction channels, the biphasic behavior can only originate from a heterogeneity of the system that influences the total reaction rate. The most probable source of the heterogeneity is the occurrence of geminate and nongeminate radical encounters. Such a behavior is predicted by computer simulation of the decay of radical pairs assuming random walk in an infinite NaX lattice (isostructural with NaY) by Johnston et al.[26] The calculations indicate that about half of the geminate radicals do not re-encounter, but rather, undergo nongeminate processes that occur on a much longer time scale. Hence, we assign the fast decay with a 1/e time of 24 μs to the reaction of geminate HCO and CH_2OH radicals that separate from the supercage in which they were generated but re-encounter and react before they have an opportunity to escape the shared diffusion sphere. On the other hand, radicals that escape the geminate diffusion sphere will ultimately react with a partner of another photolyzed precursor.

The explanation of the biphasic decay kinetics in terms of geminate and nongeminate encounters is supported by estimates of the spatial and temporal aspects of these processes. The initial intensity of the HCO band at 1847 cm^{-1} is 2.2 times larger than that of the C=O stretch of CH_3CO radical in NaY reported previously.[1,2] For the latter, we have been able to determine the extinction coefficient based on the measurement of the concentration of final products.[2] Assuming the same extinction coefficient for HCO radical, we calculate that each laser photolysis pulse generates 9×10^{15} radical pairs per cm^3. Hence, the average separation between photolyzed precursors is about 600 Å. At the same time, we are able to estimate the extent of the subspace in which geminate HCO and CH_2OH encounters occur, because the problem of geminate reaction in a finite subspace of the zeolite crystallites is closely connected with the known problem of the survival of a random walker in a finite 3-dimensional lattice with a single trap.[27,28] By analogy to our previous analysis of the acetyl radical decay in zeolite

SCHEME 1

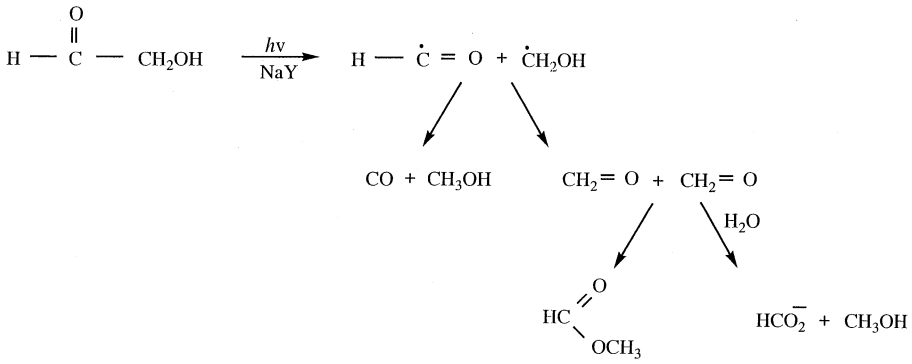

NaY[2], we assume that the average number of hops required for the random walker in the 3-dimensional cubic lattice to be trapped is 1.5 times the number of site in the lattice.[29] With a center-to-center distance of 13 Å between adjacent supercages,[30] we calculate by aid of the Einstein relation[31] $t = \langle r^2(t)\rangle/6D$ a cage-to-cage hopping time of 0.9 ns. For estimating the diffusion coefficient (D) of HCO, we assume that it is close to the measured value of $CH_2{=}CH_2$ at 298 K, $D = 3.2 \times 10^{-10}$ m^2 sec^{-1}, because the two species have similar size, shape, and degree of unsaturation[32] (a similar estimate of the diffusion coefficient of CH_2OH radical, based on $D = 1.3 \times 10^{-11}$ m^2 sec^{-1} for CH_3OH at 293 K[33] suggests that the hydroxymethyl radical is the much less mobile partner, and hence explores a smaller local environment than HCO). Therefore, the HCO radical performs 2.7×10^4 jumps, or probes on average 1.8×10^4 supercages during the 24 μs geminate reaction time. The total volume taken up by 1.8×10^4 supercages is 3.2×10^7Å,^{3} which corresponds to a sphere of 200 Å radius.[30] Hence, the time frame of geminate encounters coincides with the time it takes for a radical to approach the diffusion sphere of an adjacent radical pair. This supports our assignment of the fast component of the radical decay to the reaction of geminate HCO + CH_2-OH pairs.

On the other hand, nongeminate encounters of the radicals are expected to follow a second-order rate law[26] described by[35]

$$R_t = \frac{R_o}{1 + k_2 t R_o}$$

$$k_2 = 8\pi D\rho$$

R_o is the initial concentration of the radicals that escaped geminate reaction, k_2 is the bimolecular reaction rate constant, D is the sum of the diffusion coefficients of HCO and CH_2OH radical in the zeolite, 3.3×10^{-10} m^2 sec^{-1}, and ρ is the reaction radius. The supercage radius of 6 Å is taken as the reaction radius.[30] According to the values of these parameters, k_2 is estimated to be 5×10^{-12} cm^3 molecule^{-1} sec^{-1}, or 3×10^9 l mol^{-1} sec^{-1}. This is close to the value of k_2 derived from the least-squares fit presented in Section III, where k_2' was determined as 4.5×10^8 sec^{-1}. The latter is related to k_2 by $k_2 = \epsilon\, l\, k_2'$ (ϵ, infrared extinction coefficient of the 1847 cm^{-1} C═O stretch absorption; l, optical path length). The extinction coefficient of the CO mode is of the order of 100 L mol^{-1} cm^{-1},[36] and the thickness of the zeolite wafer is 100 μm. Hence, ϵ l is around 1 L mol^{-1} cm^{-1}, and the fit of the experimental data yields a value for k_2 of 5×10^8 L mol^{-1} sec^{-1}. This is close to the collision-controlled value predicted by the model for nongeminate encounters. We conclude that the two observed components of the HCO decay coincide with the predicted kinetics for geminate and nongeminate reaction of HCO with CH_2OH radicals. It is possible that, in addition, the slow decay contains a contribution from self-reaction of HCO radicals, assuming that CO + CH_2═O are the products. The kinetics of this nongeminate channel would not be experimentally distinguishable from the nongeminate HCO + CH_2OH channel, because the diffusion constants involved are the same within less than a factor of 2.

There are striking similarities as well as differences between the kinetic behavior of the HCO + CH_2OH system in NaY on one hand, and on the other, the CH_3CO + *tert* butyl radical or CH_3CO + naphthoxy radical systems in the same zeolite reported previously (precursors pinacolone and 1-naphthyl acetate, respectively).[1,2] When monitoring the CO stretch of the acetyl radical by step-scan FT-IR spectroscopy, we found that, like for the formyl radical, the infrared signal survives on the tens to hundreds of μs time scale. This suggests that quantitative separation of radical pairs generated by photodissociation of a precursor in zeolite Y is a more general behavior, rather than an exception. At the same time, there is an important difference in the decay kinetics of the formyl radical and acetyl radical, in that no second-order behavior is observed in the case of CH_3-CO + $(CH_3)_3C$ or CH_3CO + $C_{10}H_2O$. In fact, the acetyl radical decay is best described by a single-exponential law with a 1/e time of 71 μs (1-naphthyl acetate precursor) and 315 μs (pinacolone precursor).[1,2] Assuming that the decay of the radical, as in the case of HCO, is dictated by random walk following separation from the supercage in which photolysis took place, the absence of a flat tail implies that the radicals are not subject to nongeminate encounters. This indicates that the radical fragments of a photolyzed precursor are unable to diffuse sufficiently far to penetrate the diffusion sphere of a neighboring radical pair. We believe that an important factor responsible for the much shorter diffusion range in the acetyl radical systems is the low mobility of the relatively bulky 1-naphthyl acetate and pinacolone precursors.[2] As discussed previously in more detail, the much more abundant and orders of magnitude more slowly diffusing 1-naphthyl acetate or pinacolone molecules substantially reduce the diffusion coefficient of small, mobile species such as the acetyl radical.[2,32] The decreased diffusivity of CH_3CO in the presence of these relatively large precursors is a percolation effect due to increased tortuosity of the diffusion path by blockage of passages, in particular through the windows interconnecting the supercages.[32,37] As a result, the random walking radicals are prevented from exploring the entire volume of the zeolite crystallite, and are confined to subspaces (pockets). These are too small for nongeminate encounters to occur. A calculation presented in our previous work,[2] similar to the one described above for the HCO radical, confirms that the size of the pockets explored by diffusing CH_3CO is far too small to

permit nongeminate radical encounters to take place, consistent with the observed single-exponential decay characteristic of a geminate radical reaction. Moreover, the substantial cationic character that the CH_3CO radical assumes in the high electrostatic field environment of NaY, manifested by the strong blue shift of the CO stretch[1,2] may considerably reduce the diffusion rate compared to HCO. This almost certainly reduces further the diffusion sphere of CH_3CO radicals compared to HCO and contributes to the absence of nongeminate encounters in the case of acetyl radical systems.

Conclusions

The detection of HCO radicals in zeolite NaY by step-scan FT-IR spectroscopy has revealed an unexpectedly long lifetime at room temperature. The radicals survive on the microsecond time scale, which implies that the geminate radical pairs separate quantitatively from the supercage in which precursor photolysis took place. The decay is biphasic, independent of the precursor used. For the glycolaldehyde precursor, the final products recorded by static FT-IR spectroscopy indicate that they exclusively involve reactions of HCO and CH_2OH radicals. This allowed us to assign the biphasic decay to geminate and nongeminate radical encounters. This is the first direct kinetic observation of these two types of radical reactions in a zeolite.

Acknowledgment. This work was supported by the Director, Office of Science, Office of Basic Energy Sciences, Chemical Sciences, Geosciences and Biosciences Division of the U.S. Department of Energy under Contract No. DE-AC03-76SF00098. The authors thank Dr. Sergey Vasenkov, now at the University of Leipzig, for performing the initial experiments on the acetaldehyde photolysis, and Prof. Georgi N. Vayssilov, University of Sofia, for insightful discussions.

References and Notes

(1) Vasenkov, S.; Frei, H. *J. Am. Chem. Soc.* **1998**, *120*, 4031.
(2) Vasenkov, S.; Frei, H. *J. Phys. Chem. A* **2000**, *104*, 4327.
(3) Vasenkov, S.; Frei, H. In *Molecular and Supramolecular Photochemistry*; V. Ramamurthy, K. S. Schanze, Eds.; Marcel Dekker: New York, 2000; Vol 5, p 299.
(4) Yeom, Y. H.; Frei, H. *J. Phys. Chem. A* **2001**, *105*, 5334.
(5) Yates, J. T., Jr.; Cavanagh, R. R. *J. Catal.* **1982**, *74*, 97.
(6) Sun, H.; Frei, H. *J. Phys. Chem. B* **1997**, *101*, 205.
(7) Niki, H.; Maker, P. D.; Savage, C. M.; Hurley, M. D. *J. Phys. Chem.* **1987**, *91*, 2174.
(8) Sodeau, J. R.; Lee, E. K. C. *Chem. Phys. Lett.* **1978**, *57*, 71.
(9) Michelsen, H.; Klaboe, P. *J. Mol. Struct.* **1969**, *4*, 293.
(10) Yaylayan, V. A.; Harty-Majors, S.; Ismail, A. A. *Carbohydr. Res.* **1998**, *309*, 31.
(11) Bacher, C.; Tyndall, G. S.; Orlando, J. J. *J. Atm. Chem.* **2001**, *39*, 171.
(12) Beeby, A.; Mohammed, D. B. H.; Sodeau, J. R. *J. Am. Chem. Soc.* **1987**, *109*, 857.
(13) Ulagappan, N.; Frei, H. *J. Phys. Chem. A* **2000**, *104*, 490.
(14) Ulagappan, N.; Frei, H. *J. Phys. Chem. A* **2000**, *104*, 7834.
(15) Hirota, E. *J. Mol. Struct.* **1986**, *146*, 237.
(16) Ewing, G. E.; Thompson, W. E.; Pimentel, G. C. *J. Chem. Phys.* **1960**, *32*, 927.
(17) Milligan, D. E.; Jacox, M. E. *J. Chem. Phys.* **1964**, *41*, 3032.
(18) Moore, J.; Pearson, K. *Kinetics and Mechanism*, 3rd ed.; Wiley: New York, 1981; p 19.
(19) Seifert, K. G.; Bargon, J. *Angew. Chem.* **1973**, *85*, 768.
(20) Bagott, J. E.; Frey, H. M.; Lightfoot, P. D.; Wash, R. *J. Phys. Chem.* **1987**, *91*, 3386.
(21) Yadav, J. S.; Goddard, J. D. *J. Chem. Phys.* **1986**, *84*, 2682.
(22) Horowitz, A.; Kershner, C. J.; Calvert, J. G. *J. Phys. Chem.* **1982**, *86*, 3094.
(23) Horowitz, A.; Calvert, J. G. *J. Phys. Chem.* **1982**, *86*, 3105.
(24) Gill, R. J.; Atkinson, G. H. *Chem. Phys. Lett.* **1979**, *64*, 426.
(25) Tachikawa, H.; Ohta, N. *Chem. Phys. Lett.* **1994**, *224*, 465.
(26) Johnston, L. J.; Scaiano, J. C.; Shi, J. L.; Siebrand, W.; Zerbetto, F. *J. Phys. Chem.* **1991**, *95*, 10018.
(27) Weiss, G. H.; Havlin, S.; Bunde, A. *J. Stat. Phys.* **1985**, *40*, 191.
(28) Den Hollander, W. T. F. *J. Stat. Phys.* **1985**, *40*, 201.
(29) Musho, M. K.; Kozak, J. J. *J. Chem. Phys.* **1984**, *81*, 3229.
(30) Breck, D. W. *Zeolite Molecular Sieves; Structure, Chemistry, and Use*; Wiley: New York, 1974; p 177.
(31) Karger, J.; Ruthven, D. M. *Diffusion in Zeolites and Other Microporous Solids*; Wiley: New York, 1992; p 25.
(32) Nivarthi, S. S.; Davis, H. T.; McCormick, A. V. *Chem. Eng. Sci.* **1995**, *50*, 3217.
(33) Grenier, P.; Meunier, F.; Gray, P. G.; Karger, J.; Xu, Z.; Ruthven, D. M. *Zeolites* **1994**, *14*, 242.
(34) Brandani, S.; Ruthven, D. M.; Karger, J. *Zeolites* **1995**, *15*, 494.
(35) Moore, J.; Pearson, K. *Kinetics and Mechanism*, 3rd ed.; Wiley: New York, 1981; p 238.
(36) Bellamy, L. J. *The Infrared Spectra of Complex Molecules*, 3rd ed.; Chapman and Hall: London, 1975; p 176.
(37) Keffer, D.; McCormick, A. V.; Davis, H. T. *J. Phys. Chem.* **1996**, *100*, 967.